

**LA-UR-13-25755**

Approved for public release; distribution is unlimited.

**Title:** Summary of pre-shot Lasnex simulations in support  
of shock/shear experiments at NIF

**Author(s):** Devolder, Barbara G.

**Intended for:** Report

**Issued:** 2013-07-23



**Disclaimer:**

Los Alamos National Laboratory, an affirmative action/equal opportunity employer, is operated by the Los Alamos National Security, LLC for the National Nuclear Security Administration of the U.S. Department of Energy under contract DE-AC52-06NA25396. By approving this article, the publisher recognizes that the U.S. Government retains nonexclusive, royalty-free license to publish or reproduce the published form of this contribution, or to allow others to do so, for U.S. Government purposes.

Los Alamos National Laboratory requests that the publisher identify this article as work performed under the auspices of the U.S. Department of Energy. Los Alamos National Laboratory strongly supports academic freedom and a researcher's right to publish; as an institution, however, the Laboratory does not endorse the viewpoint of a publication or guarantee its technical correctness.

## **Summary of pre-shot Lasnex simulations in support of shock/shear experiments at NIF**

Barbara DeVolder, XCP-6

July 22, 2013

### **Abstract**

This report describes Lasnex simulations to characterize the laser drive and halfraum dynamics for upcoming shock/shear experiments at NIF. Synthetic diagnostics, such as Dante 1 and backscatter, are also included.

### Halfraum and foam package geometry

Although the planned shock/shear experiments are three-dimensional and include two halfraums, Lasnex simulations that include one halfraum, that evaluate the halfraum dynamics (such as Dante temperature and peak stagnation pressure), and that provide frequency-dependent flux sources for RAGE calculations of the foam package are adequate for pre-shot design and post-shot analysis. Figure 1 shows one halfraum, with the laser entrance hole (LEH) at the right, and part of the designed foam package. Certain design details of the foam package are omitted in Lasnex simulations, but these should not affect the halfraum dynamics or the flux sources at the upstream end of the package.

As depicted in Figure 1, the gold wall of the halfraum is 100  $\mu\text{m}$  thick, the radius of the LEH is 1.3 mm, the axial length of the halfraum is 3.0 mm, and the radius of the halfraum is 2.0 mm. The gas-fill density is 1.0e-6 g/cc; the density of the gold wall is 19.3 g/cc. CH foam is used at two densities: the ablator and foam wall (colored yellow) density is 1.0 g/cc; the foam fill (light green) density is 60 mg/cc. The ablator thickness is 270  $\mu\text{m}$ , the radius of the foam fill is 750  $\mu\text{m}$ , and the foam wall thickness is 250  $\mu\text{m}$ ; these are as-built dimensions. Due to the setup of the Lasnex mesh, created by Evan Dodd, the thicknesses of the gold wall and the high-density foam wall are “hard-wired” to be equal. Therefore, in the interest of accurately simulating the halfraum, we set the foam wall thickness to 100  $\mu\text{m}$ , i.e., to the as-built gold-wall thickness. The constraint that the foam and gold walls must have the same thickness is one that should be removed in future simulations, to allow accurate (although only two-dimensional) modeling of the foam package. Modifying the Lasnex input file to relax this constraint involves reconstructing the mesh, and this is non-trivial.

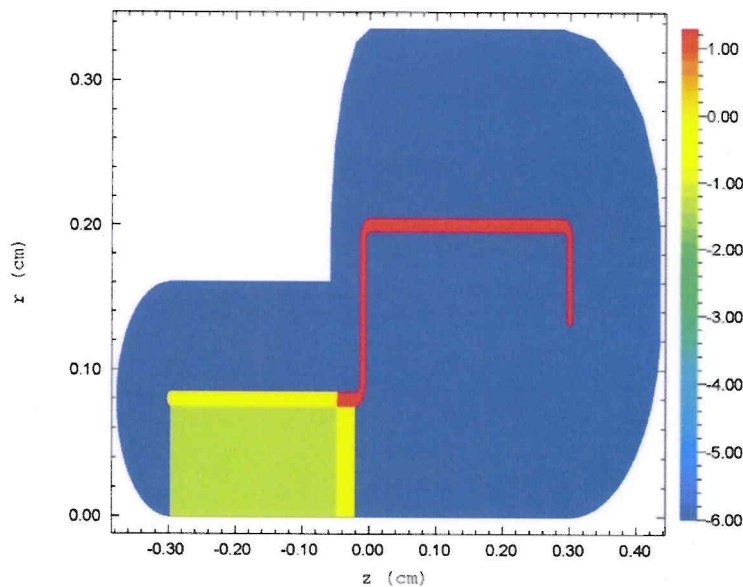


Figure 1. Geometry and initial densities (colored as log values of densities, g/cc) for halfraum and foam package. (The r and z axes are not to the same scale.)

## Halfraum dynamics

The role of Lasnex simulations in the design of shock/shear experiments at NIF is to evaluate the performance of the halfraum, including stagnation pressure on axis and Dante temperatures, and to provide a frequency-dependent flux source for use in 3-D Rage simulations of the foam package. To address variations in the laser power and energy delivered to the halfraum, we studied the effects of varying the baseline laser energy by +/- 10%. The baseline laser pulse is a scaled version of John Kline's initial proposal for Fanbolt, given in Appendix 1. The baseline modifications for shock/shear were to scale the times by 3.0 and the powers by 0.30. In all simulations, the laser power is divided equally between the 44.5 and 50 degree cones. Figure 2 illustrates the three laser power profiles (baseline, +/- 10%) and also indicates the total laser energy delivered.

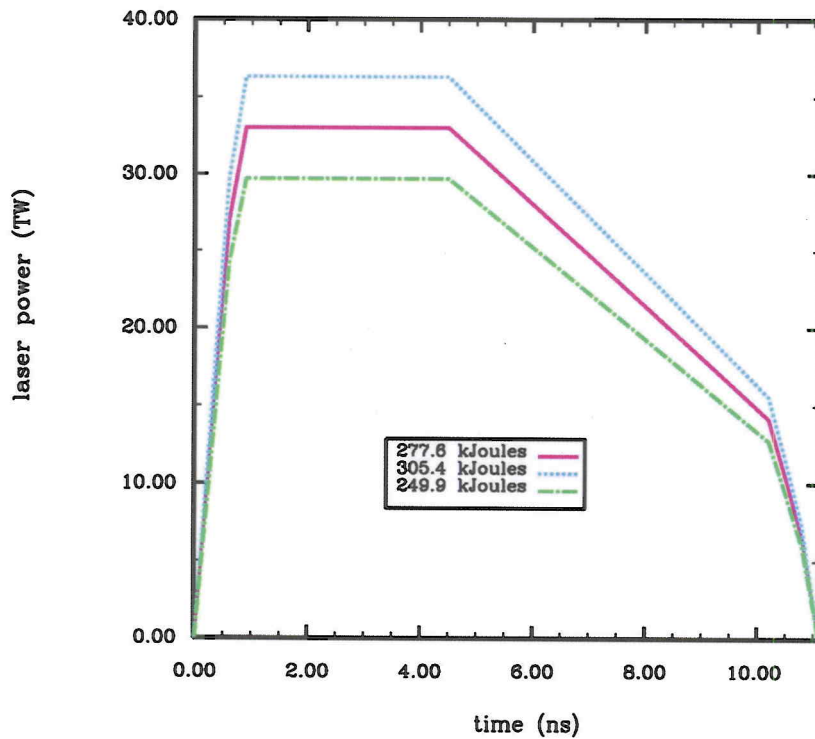


Figure 2. Laser power and laser energy used in Lasnex simulations, for three cases: baseline (scaled Fanbolt) and +/- 10% change in baseline laser energy.

Table 1 summarizes the differences in laser energy, peak pressure on axis, and peak Dante 1 radiation temperature  $T_r$  for three Lasnex simulations that used the three laser power profiles of Figure 2. Because two types of averaging are valid for simulated Dante temperatures, both are presented for each simulation. Peak Dante temperatures occur in the range of 4.45 – 4.85 ns. Peak pressures occur at ~ 12 – 13 ns (+/- 1 ns).

Table 1. Comparison of stagnation pressure and Dante temperature for varying laser energies

	Baseline laser energy	Increase laser energy by 10%	Decrease laser energy by 10%
Laser energy	277.6 kJoules	305.4 kJoules	249.9 kJoules
Peak pressure on axis	140.7 Mbar	162.1 Mbar	136.0 Mbar
Peak Dante Tr (37 degrees)	248.7 – 252.3 eV	253.6 – 257.9 eV	242.1 – 245.3 eV

Synthetic diagnostics: Dante 1 Tr

Synthetic diagnostics, such as Dante temperatures and backlighters, can be calculated with a Yorick post-processing script developed by Ian Tregillis. The script, which uses Lasnex output files, assumes a Planckian blackbody distribution in calculating Dante 1 Tr; this is a reasonable assumption for hohlraums. Below is the Dante 1 time history for the halfraum, using the baseline laser pulse.

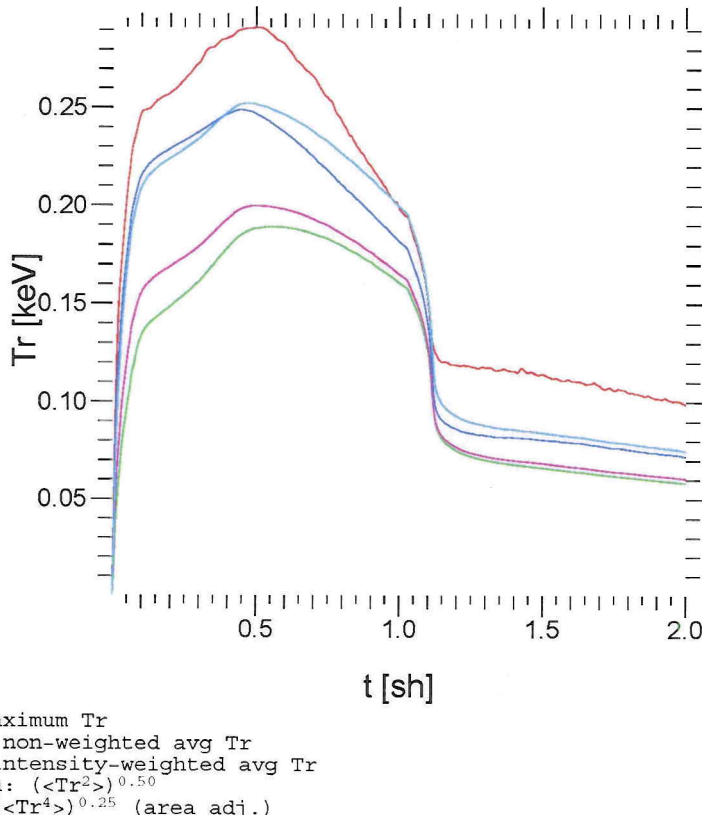


Figure 3. Dante 1 Tr vs time (37 degrees), post-processed from Lasnex output, for several averaging methods. The blue and cyan curves have been shown, in other contexts, to have best agreement with data. Baseline laser drive was used in the Lasnex simulation.

Several averaging methods are illustrated in Figure 3, but only the intensity-weighted average Tr (blue curve) and the rms fourth root Tr (cyan curve) have been shown (for other applications) to be credible when comparing with data. Therefore, we interpret synthetic Dante Tr profiles as predicting a peak Tr close to 250 eV (see Table 1) at 0.5 shake, and a rapid decline to less than 100 eV beyond 11 ns.

However, comparing synthetic Dante 1 (37 degrees) of Figure 3 with Lasnex output for the halfraum Tr reveals a discrepancy at late times (after the laser is turned off). Figures 4 and 5 depict solid contour plots of the entire geometry (halfraum and foam package) at 0.5 shake (the time of peak synthetic Dante 1 Tr, from Figure 3) and 1.8 shakes (at which time synthetic Dante 1 Tr has fallen to about 75 eV). The contour plots of Figure 4 show qualitative agreement with the synthetic Dante temperature at 0.5 shake: the peak Tr in the halfraum is 250 eV near the laser entrance hole. At late times, however, the difference between synthetic Dante Tr and Lasnex output is significant (and, currently, is an unresolved issue): synthetic Dante temperatures (blue and cyan curves) are less than 100 eV after the laser is turned off at 11.1 ns; but Figure 5 shows temperatures throughout the halfraum that are greater than 100 eV. At present, we do not have an explanation for this discrepancy.

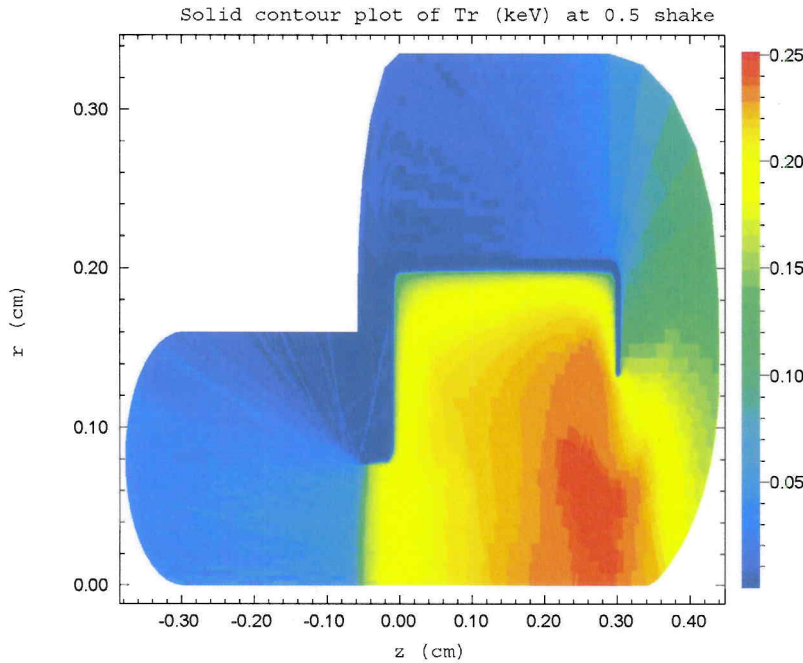


Figure 4. Solid contour plot of Tr at 0.5 shake for the halfraum and foam package, calculated directly from Lasnex. Baseline laser drive was used in this Lasnex simulation.

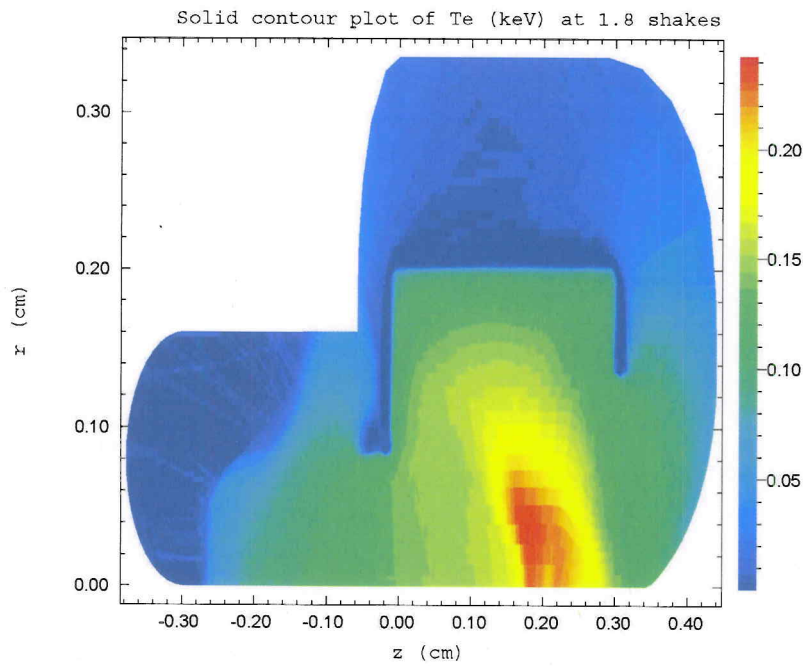


Figure 5. Solid contour plot of  $T_e$  at 1.8 shakes for the halfraum and foam package, calculated directly from Lasnex. Baseline laser drive was used in this Lasnex simulation.

#### Stagnation pressure: peak pressure on-axis

Peak pressures on-axis occur at 12 – 13 ns, with values indicated in Table 1. For illustration, Figure 6 is a solid contour plot of pressure at 12 ns for the baseline laser drive. The peak pressure occurs at  $z \sim 0.19$  cm, with a value of  $\sim 141$  Mbar.

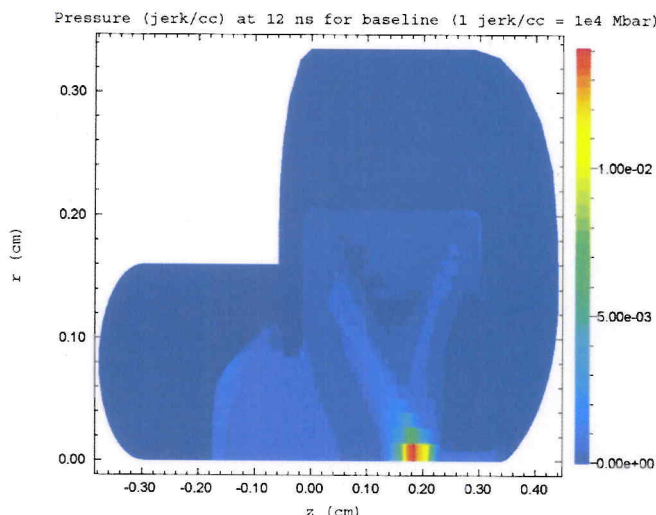


Figure 6. Solid contour plot of pressure at 12 ns for the halfraum and foam package.

### Synthetic diagnostics: backlighter

The first NIF shot for the shock/shear campaign is scheduled for August 6 and will be a backlighter-only shot to demonstrate that the large-area backlighter will meet experimental requirements before fielding the first imaging shot with the target. John Kline notes that this area backlighter will be one of the largest ever shot, generating a  $2.3 \times 3$  mm spot using 24 NIF beams and 132 kJoules of energy. One set of simulations requested by the experimentalists was related to the effect of changing the prepulse (or picket) in the laser drive on the backlighter foil (Fe, 12.7  $\mu\text{m}$  thick). The simulations became part of a “picket playbook” for the planned backlighter shot. The results are presented in Figures 7 – 11.

Using the laser drive provided by Kirk Flippo as the baseline, we scaled his prepulse peak power by 0 (actually, a small nonzero value),  $\frac{1}{2}$ , and 2. Figure 7 shows the laser drives on the backlighter foil for these four cases. Also noted in the figure is the total energy delivered for each drive (which is the area under the power/beam curve—including the prepulse and the main pulse—multiplied by 22 beams).

**Varying prepulse for backlighter drive BL-3ns-1.8TW  
(energies derived by multiplying areas by 22 beams)**

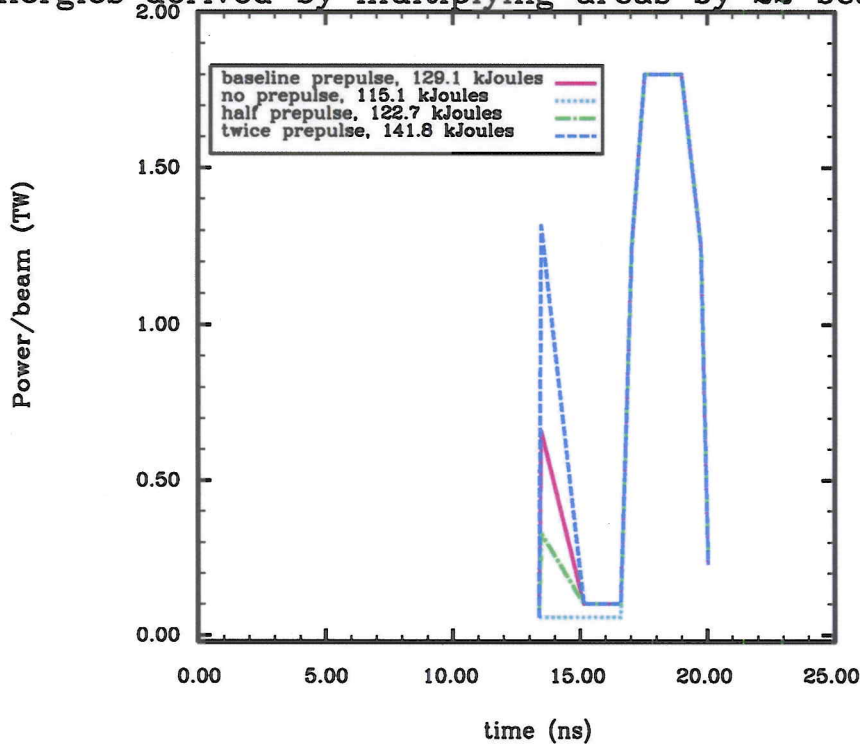


Figure 7. Varying prepulse laser power profiles for the planned backlighter shot at NIF.

Figures 8 – 11 depict emitted flux as a function of bin energy ( $\text{jerks}/\text{cm}^2/\text{steradian}/\text{keV}$ , as a function of energy in keV). (The conversion is 1 jerk =  $1\text{e}9$  Joules.) In each figure, each individual curve is at a specific time, and the range in times extends over the entire time of the laser pulse—13.4 to 20.0 ns. The major difference among the four cases is observed in the “no prepulse” case.

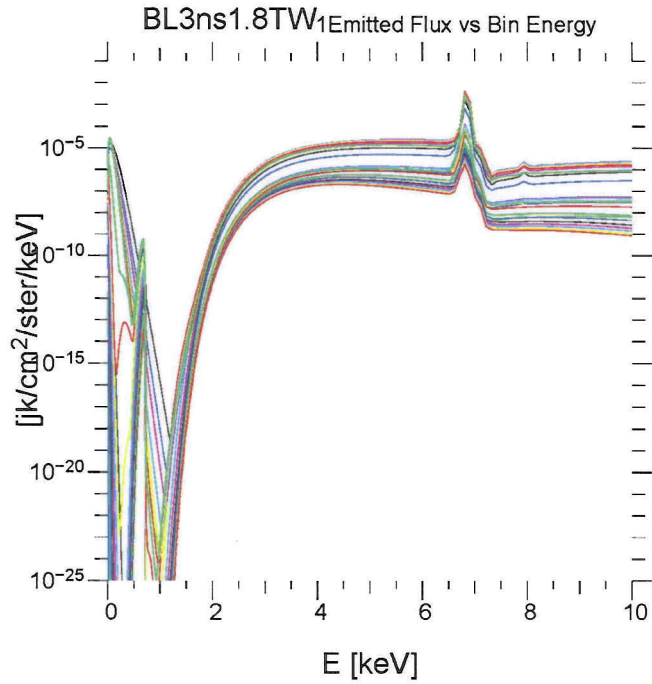


Figure 8. Emitted flux vs bin energy for times between 13.4 and 20.0 ns. This is the baseline case, for which the laser energy is 129.1 kJoules.

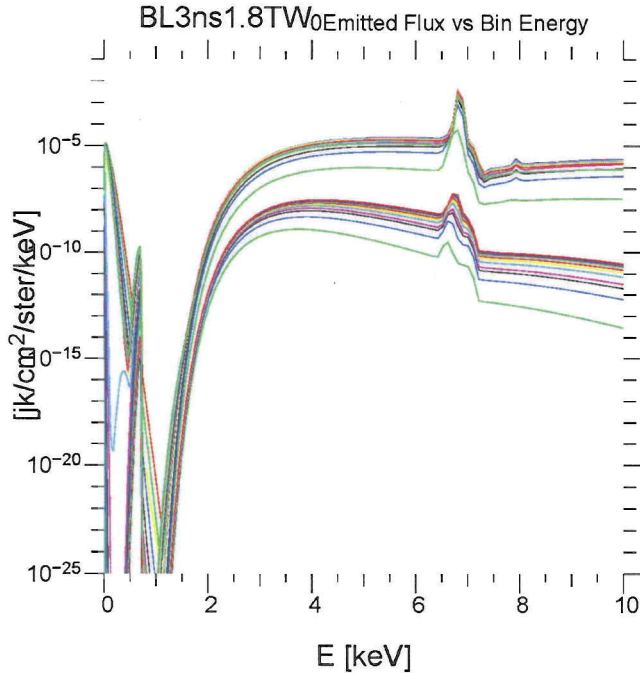


Figure 9. Emitted flux vs bin energy for times between 13.4 and 20.0 ns. This is the “zero picket” case, for which the laser energy is 115.1 kJoules.

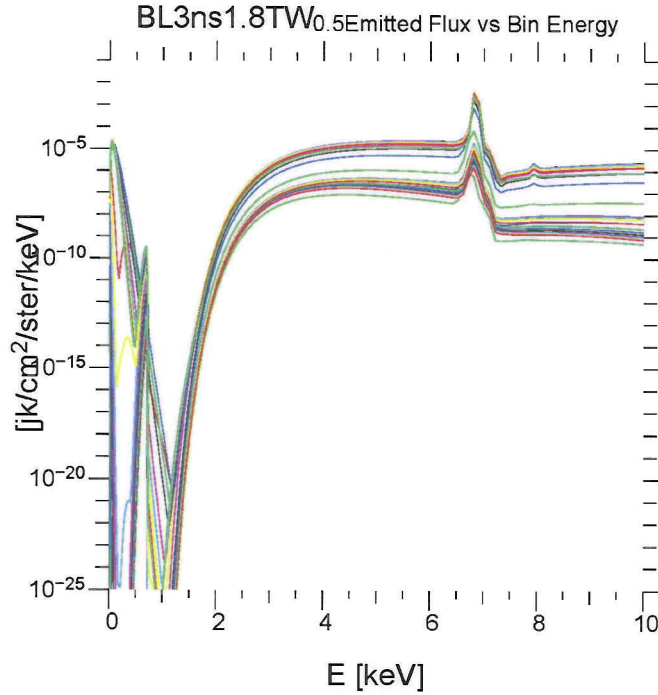


Figure 10. Emitted flux vs bin energy for times between 13.4 and 20.0 ns. This is the “half picket” case, for which the laser energy is 122.7 kJoules.

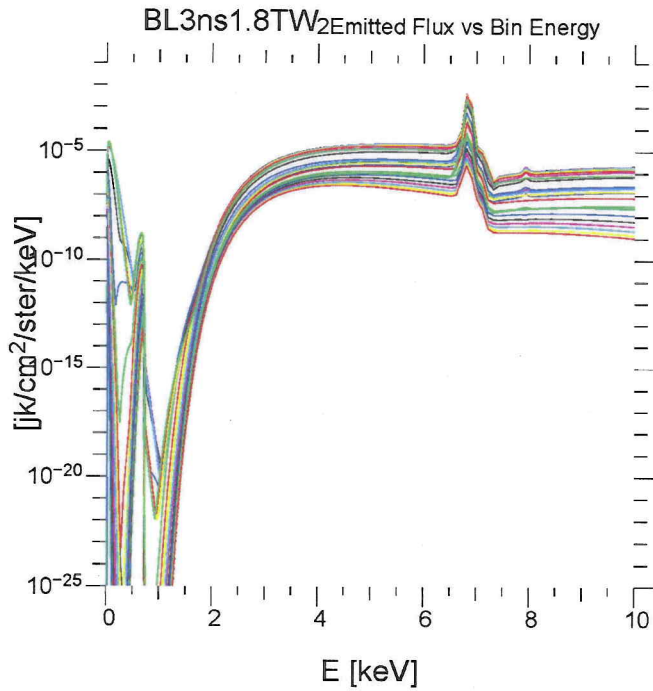


Figure 11. Emitted flux vs bin energy for times between 13.4 and 20.0 ns. This is the “twice picket” case, for which the laser energy is 141.8 kJoules.

To examine the four cases on one plot at a time corresponding to the center of the flat-top main pulse, we co-plotted emitted flux as a function of energy at 18.3 ns. These are shown in Figures 12 and 13, which are the same plot except that the abscissa of Figure 13 extends only to 2 keV. Differences among

the four cases are evident only at low energies ( $< 2$  keV), but the quantitative values of these differing fluxes are very small compared with the peak flux at  $\sim 6.8$  keV.

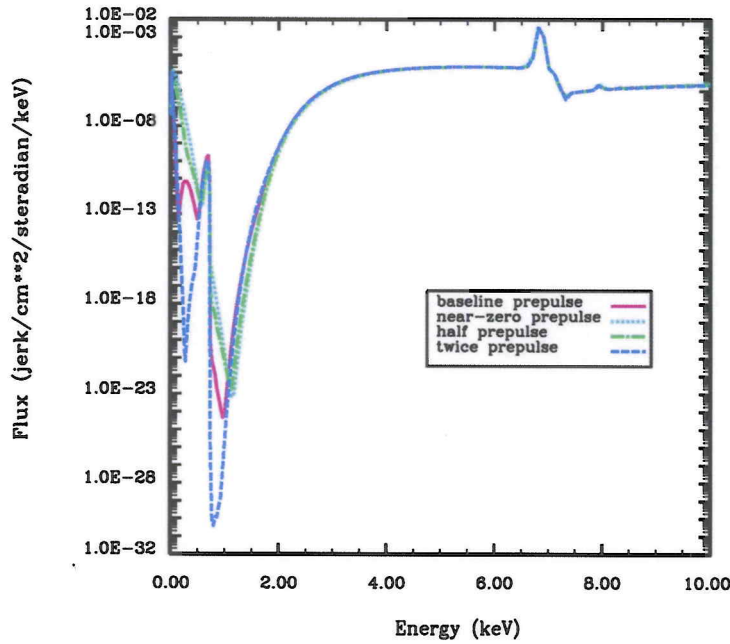


Figure 12. Emitted flux vs bin energy at 18.3 ns, for four cases of the “picket playbook.” Energy range is between 0 and 10 keV.

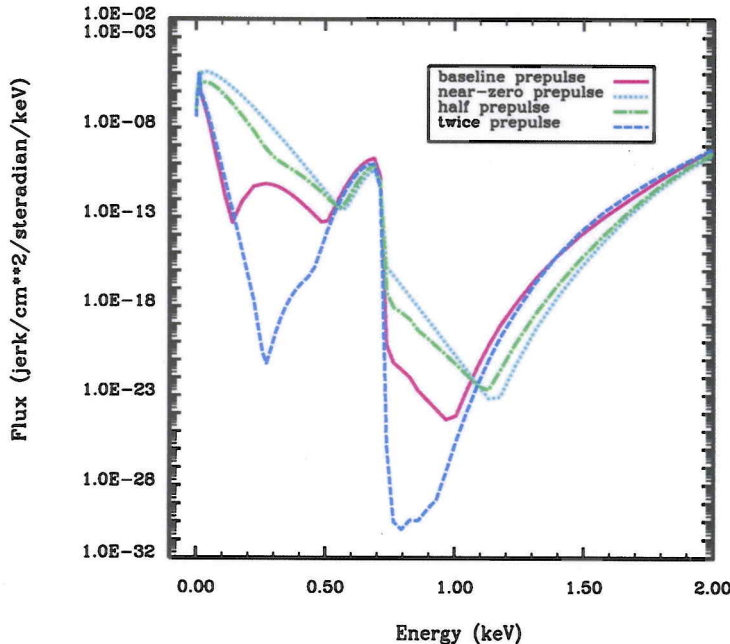


Figure 13. Emitted flux vs bin energy at 18.3 ns, for four cases of the “picket playbook.” Energy range is between 0 and 2 keV.

### Qualitative discussion of possible errors and uncertainties in Lasnex simulations

There are at least three sources of uncertainties or errors that could adversely affect comparisons with data: (1) the constraint on the Lasnex mesh that requires the gold and foam wall thicknesses to be equal may preclude accurate predictions; (2) the time of switching to an Eulerian mode affects some of the physics; (3) Lagrangian mesh motion results in changes to the position of the surface used to calculate a frequency-dependent flux source for Rage simulations of the foam package. Each of these factors can be explored in quantitative detail in post-shot simulations of the first shock/shear experiments at NIF.

The Lasnex mesh, provided by Evan Dodd, has the advantage of a sufficiently large number of zones in the near-vacuum halfraum, so that the calculation can be switched to an Eulerian mode at a relatively early time (1 – 2 ns). (For a setup that coarsely zones the low density gas at t=0, the simulation must be run in Lagrangian mode for a long enough time to allow the finely-zoned gold wall to fill the halfraum; this longer time generally means that extensive rezoning must be done during the Lagrangian phase. Evan's zoning avoids the need for manual rezoning.) The disadvantage of Evan's mesh is that the gold and foam walls for the halfraum and the package, respectively, are constrained to have the same thickness. In the shock/shear design, the gold wall thickness is 100  $\mu\text{m}$  and the foam wall thickness is 250  $\mu\text{m}$ . The current specification of the mesh in the input file precludes the ability to use different thicknesses. Instead, the simulations described in this report used the correct gold wall thickness and an incorrect foam wall thickness, in an attempt to correctly model the halfraum. This situation may affect halfraum dynamics, shock behavior in the package, and the fds source provided for Rage simulations. Future work may allow the flexibility to use different wall thicknesses for the gold and the foam, but such modifications are non-trivial to make.

As described above, the advantage of Evan's mesh is to allow a switch at a relatively early time to an Eulerian mode, thus avoiding the need for extensive manual rezoning. However, the choice of such a switch time affects the physics results of the simulations. For example, we have noted differences on the order of 15% in the radiation fluence (energy) flowing from the halfraum to the foam package. The optimum choice of a switch time may be determined once data is obtained.

The contour in Lasnex simulations that is used to calculate an fds source for Rage simulations of the foam package is the boundary separating the halfraum from the upstream side of the foam package. During the Lagrangian phase of the Lasnex simulation, that contour may move. Therefore, the fds source surface in Lasnex may not be located at the same position as that in Rage, which is an Eulerian AMR code.

### Acknowledgements

I thank Evan Dodd for providing a Lasnex input file that could be readily adapted to the shock/shear simulations. I thank Ian Tregillis for providing his synthetic diagnostics script for Dante and backscatter calculations. I acknowledge useful discussions with Ian and with Forrest Doss.

Appendix 1: John Kline's initial proposal for Fanbolt power profile

John Kline distributed the following power profile on April 19, 2012, as an initial proposal for use in Fanbolt experiments at NIF. This pulse shape was modified for use in pre-shot Lasnex simulations of shock/shear experiments planned at NIF, by applying constant scale factors to the times and powers: 3.0 and 0.30, respectively. That is, the power profile was extended in time and reduced in magnitude. Extending the time for the laser pulse was necessary, because shock/shear experiments at NIF are designed to look at late-time ( $\sim 20$  ns) physics, after the laser is turned off.

<u>Time (ns)</u>	<u>Power (TW)</u>	<u>Energy (kJoule)</u>
0	0	0
0.1	45	4.5
0.2	90	13.5
0.3	110	24.5
0.4	110	35.5
0.5	110	46.5
0.6	110	57.5
0.7	110	68.5
0.8	110	79.5
0.9	110	90.5
1	110	101.5
1.1	110	112.5
1.2	110	123.5
1.3	110	134.5
1.4	110	145.5
1.5	110	156.5
1.6	106.7	167.17
1.7	103.4	177.51
1.8	100.1	187.52
1.9	96.8	197.2
2	93.5	206.55
2.1	90.2	215.57
2.2	86.9	224.26
2.3	83.6	232.62
2.4	80.3	240.65
2.5	77	248.35
2.6	73.7	255.72
2.7	70.4	262.76

<u>Time (ns)</u>	<u>Power (TW)</u>	<u>Energy (kJoule)</u>
2.8	67.1	269.47
2.9	63.8	275.85
3	60.5	281.9
3.1	57.2	287.62
3.2	53.9	293.01
3.3	50.6	298.07
3.4	47.3	302.8
3.5	35	306.3
3.6	22	308.5
3.7	0	308.5